Synthesis and Catalytic Performance of Pd Nanoparticle/Functionalized CNF Composites by a Two-Step Chemical Vapor Deposition of Pd(allyl)(Cp) Precursor

ARTICLE *in* CHEMISTRY OF MATERIALS · JUNE 2009

Impact Factor: 8.35 · DOI: 10.1021/cm8031225

8 AUTHORS, INCLUDING:

Changhai Liang
Dalian University of Technology
137 PUBLICATIONS **3,813** CITATIONS
SEE PROFILE

Yuemin Wang
Ruhr-Universität Bochum
99 PUBLICATIONS **2,431** CITATIONS
SEE PROFILE

Synthesis and Catalytic Performance of Pd Nanoparticle/Functionalized CNF Composites by a Two-Step Chemical Vapor Deposition of Pd(allyl)(Cp) Precursor

Changhai Liang,*[,†,‡] Wei Xia,[†] Maurits van den Berg,[†] Yuemin Wang,[†] Hamideh Soltani-Ahmadi,[†] Oliver Schlüter,[†] Roland A. Fischer,[§] and Martin Muhler*[,†]

Laboratory of Industrial Chemistry and Laboratory of Inorganic Chemistry II, Ruhr-University Bochum, D-44780 Bochum, Germany, and Carbon Research Laboratory, State Key Laboratory of Fine Chemicals, Dalian University of Technology, Dalian 116012, China

Received November 17, 2008. Revised Manuscript Received April 16, 2009

Pd nanoparticle/functionalized CNF composites were synthesized by a two-step chemical vapor deposition of Pd(allyl)(Cp) as precursor at atmospheric pressure. Online mass spectrometry was used to measure the gas fragments during the two-step CVD. The functionalized CNFs and the resulting composites were characterized by temperature-programmed desorption mass spectroscopy, inductively coupled plasma-optical emission spectroscopy, X-ray diffraction, and transmission electron microscopy. The catalytic hydrogenation of cyclooctene on the Pd/CNF nanocomposites was also investigated in a fixed-bed reactor at 40 °C under atmospheric pressure. No palladium deposition was observed on the raw CNFs, as a result of the absence of anchoring sites. The functionalization of CNFs with HNO_3 solution resulted in the formation of surface oxygen groups. The Pd(allyl)(Cp) precursor could be dissociatively adsorbed on the surface of the CNF by the reaction between the ligands and the surface oxygen groups. Further reduction in H_2 formed the Pd/CNF nanocomposites. The palladium loading on the functionalized CNFs depends on the degree of functionalization of the CNFs and on the amount of precursor provided. TEM and XRD results showed that highly dispersed and evenly distributed Pd particles with diameters of 2−4 nm could be prepared by this two-step CVD method. The Pd/CNF nanocomposite catalysts exhibited high activity and stability in the catalytic hydrogenation of cyclooctene, which can be attributed to the special interaction between the palladium nanoparticles and the CNFs and to the mesoporous nature of the CNFs, which prevents mass transfer limitation. The two-step CVD route has great potential in the controlled synthesis of CNF-supported metal catalysts with high dispersion and uniform distribution.

Introduction

Carbon nanotubes (CNTs) and nanofibers (CNFs) have attracted great scientific interest from a fundamental point of view as well as for their potential applications since their discovery[1] and large scale synthesis,[2,3] owing to their superior mechanical and thermal properties, unique electrical and structural characteristics, and specific adsorption properties. These novel nanostructured carbon materials can be used in conductive and high-strength composites, energy storage and energy conversion devices, sensors, field emission displays, and radiation detectors.[4−8] They have also been considered for use as catalysts or catalyst supports in heterogeneous catalysis.[9−13] Some reactions, such as hydrogenation and dehydrogenation reactions,[14−20] hydroformylation,[21−23] and electro-oxidation reactions,[24−28] have been investigated using catalysts supported on CNTs or CNFs. Those catalysts have

* To whom correspondence should be addressed. Fax: +86-411-39893991 (C.L.). E-mail: changhai@dlut.edu.cn (C.L.) or muhler@techem.ruhr-uni-bochum.de (M.M.).
† Laboratory of Industrial Chemistry, Ruhr-University Bochum.
‡ Dalian University of Technology.
§ Laboratory of Inorganic Chemistry II, Ruhr-University Bochum.

(1) Iijima, S. *Nature* **1991**, *354*, 56.
(2) Ebbesen, T. W.; Ajayan, P. M. *Nature* **1992**, *358*, 220.
(3) Li, W. Z.; Xie, S. S.; Qian, L. X.; Chang, B. H.; Zou, B. S.; Zhou, W. Y.; Zhao, R. A.; Wang, G. *Science* **1996**, *274*, 1701.
(4) Baughman, R. H.; Zakhidov, A. A.; de Heer, W. A. *Science* **2002**, *297*, 787.
(5) Andrews, R.; Jacques, D.; Qian, D.; Rantell, T. *Acc. Chem. Res.* **2002**, *35*, 1008.
(6) Subramoney, S. *Adv. Mater.* **1998**, *10*, 1157.
(7) Popov, V. N. *Mater. Sci. Eng. R.* **2004**, *43*, 61.
(8) Cheng, H. M.; Yang, Q. H.; Liu, C. *Carbon* **2001**, *39*, 1447.
(9) de Jong, K. P.; Geus, J. W. *Catal. Rev. Sci. Eng.* **2000**, *42*, 481.
(10) Cop, B.; Planeix, J. M.; Brotons, V. *Appl. Catal., A* **1998**, *173*, 175.
(11) Serp, P.; Corrias, M.; Kalck, P. *Appl. Catal., A* **2003**, *253*, 337.
(12) Zhang, J.; Liu, X.; Blume, R.; Zhang, A. H.; Schlögl, R.; Su, D. S. *Science* **2008**, *322*, 73.
(13) Pan, X. L.; Fan, Z. L.; Chen, W.; Ding, Y. J.; Luo, H. Y.; Bao, X. H. *Nat. Mater.* **2007**, *6*, 507.
(14) Planeix, J. M.; Coustel, N.; Coq, B.; Brotons, V.; Kumbhar, P. S.; Dutartre, R.; Geneste, P.; Bernier, P.; Aiayan, P. M. *J. Am. Chem. Soc.* **1994**, *116*, 7935.
(15) Mestl, G.; Maksimova, N. I.; Keller, N.; Roddatis, V. V.; Schlögl, R. *Angew. Chem., Int. Ed.* **2002**, *40*, 2066.
(16) Pham-Huu, C.; Keller, N.; Ledoux, M. J.; Charbonnière, L.; Ziessel, R. *Chem. Commun.* **2000**, *19*, 1871.
(17) Park, C.; Baker, R. T. K. *J. Phys. Chem. B* **1998**, *102*, 5168.
(18) Liang, C. H.; Li, Z. L.; Qiu, J. S.; Li, C. *J. Catal.* **2002**, *211*, 278.
(19) Baker, R. T. K.; Laubernds, K.; Wootsch, A.; Paal, Z. *J. Catal.* **2000**, *193*, 165.
(20) Ros, T. G.; Keller, D. E.; van Dillen, A. J.; Geus, J. W.; Koningsgerger, D. C. *J. Catal.* **2002**, *211*, 85.
(21) Gao, R.; Tan, C. D.; Baker, R. T. K. *Catal. Today* **1999**, *65*, 385.
(22) Giordano, R.; Serp, P.; Kalck, P.; Kihn, Y.; Schreiber, J.; Marhic, C.; Duvail, J. L. *Eur. J. Inorg. Chem.* **2003**, 610.
(23) Zhang, Y.; Zhang, H. B.; Lin, G. D.; Chen, P.; Yuan, Y. Z.; Tsai, K. R. *Appl. Catal., A* **1999**, *187*, 213.
(24) Bessel, C. A.; Laubernds, K.; Rodriguez, N. M.; Baker, R. T. K. *J. Phys. Chem. B* **2001**, *105*, 1115.

10.1021/cm8031225 CCC: $40.75
Published on Web 05/01/2009

shown superior catalytic activity and selectivity in the above-mentioned reactions, which have been attributed to their unique structure features, electronic properties, and interaction between the nanostructured support and the metal particles. However, applications of CNFs in catalysis are still in an early stage of development. Controllable synthesis routes need be explored to CNF-supported catalysts. Conventionally, CNF-supported catalysts have been prepared by various methods such as impregnation, coprecipitation, and ion exchange. Difficulties remain in controlling the preparation parameters with multistep procedures, with obtaining uniform metal particles due to solvent blocking of the adsorption sites, and in reaching high reproducibility. Chemical vapor deposition (CVD) has been widely used to prepare coatings of metals, oxides, nitrides, and carbides for semiconductor and opto-electronic applications.[29,30] This technique was also shown to be a powerful method for generating highly dispersed catalysts in a controlled and reproducible manner.[31,32]

Supported palladium catalysts have been widely used to synthesize basic chemicals and fine chemicals.[33,34] These reactions are very sensitive to the metal particle size. Generally, small palladium particles with a uniform size distribution are favorable for the activity and selectivity of the reactions. The traditional methods such as impregnation and precipitation often lead to large palladium particles and an inhomogeneous distribution.[35] Palladium has been deposited onto mesoporous MCM materials by the vapor grafting route, and the as-prepared catalysts with good dispersion showed remarkable activity in Heck reactions.[36,37] Also, palladium has been deposited onto silica supports by CVD in a fluidized-bed reactor, and highly dispersed catalysts were obtained.[38,39] A Pd film on multiwall CNTs with a buffer layer of TiC has also been prepared by CVD of $Pd(hfac)_2$, whereas isolated Pd was formed without the TiC layer.[40] However, the preparation of well-dispersed metal particles on CNFs is very challenging, as few sites are available for the anchoring of the metal organic precursors.[41−43] Herein we report the preparation and characterization of palladium nanoparticle/functionalized CNF composites by CVD of Pd(allyl)(Cp). The nanocomposite catalysts exhibit excellent activity in the hydrogenation of cyclooctene and therefore might find applications in hydrogenation reactions.

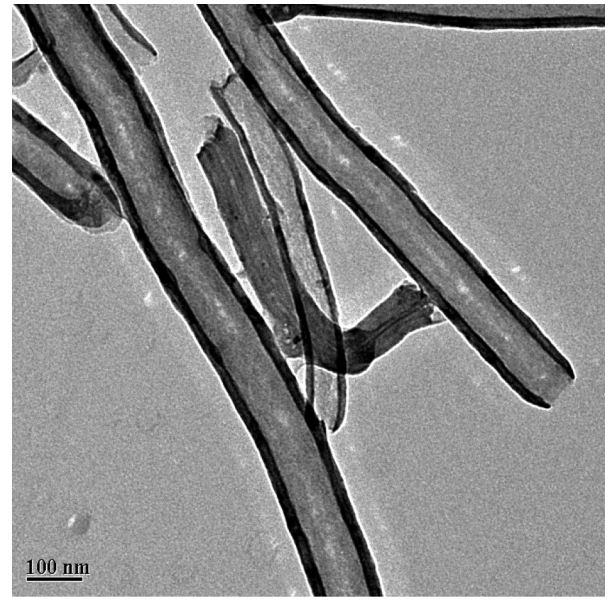

Figure 1. A representative TEM image of the raw CNFs.

Experimental Section

Raw CNFs were purchased from Applied Sciences Inc. The outer diameter of the CNFs was 70−200 nm, the length was 20−100 μm, and the BET surface area was 50−60 $m^2\ g^{-1}$. A representative TEM image of the CNFs is displayed in Figure 1. Allylcyclopentadienylpalladium [Pd(allyl)(Cp)] was synthesized by reacting $Pd_2(allyl)_2Cl_2$[44] with NaCp.[45] Pd(allyl)(Cp) was used as palladium precursor because it is stable in moist air and volatile at low temperature.[46]

To increase the amount of anchoring sites on the surface, the CNFs were functionalized at reflux with 5 M HNO_3 for 3 h. Then CNFs were filtered and washed with distilled water until the pH of the rinsing water was constant. The resulting material was dried overnight at 110 °C.

The palladium deposition onto the CNFs was carried out in a fixed-bed reactor described elsewhere.[38,43] About 0.2 g of CNF sample was filled into the reactor, and a weighted amount of precursor was transferred into the sublimator. The CNF sample was heated to 110 °C and maintained at this temperature for 2 h in a flow rate of in 70 mL min^{-1} to remove the physisorbed water prior to chemical vapor deposition. Then the reactor temperature was decreased to 80 °C. The helium carrier gas saturated with the Pd(allyl)(Cp) precursor was fed to the reactor at a flow rate of 70 mL min^{-1}, in which the adsorption of the precursor took place.

(25) Li, W. Z.; Liang, C. H.; Zhou, W. J.; Qiu, J. S.; Li, H. Q.; Sun, G. Q.; Xin, Q. *Carbon* **2004**, *42*, 436.
(26) Steigerwalt, E. S.; Deluga, G. A.; Cliffel, D. E.; Lukehart, C. M. *J. Phys. Chem. B* **2001**, *105*, 8097.
(27) Che, G. L.; Lakshmi, B. B.; Fisher, E. R.; Martin, C. R. *Nature* **1998**, *393*, 346.
(28) Vinodgopal, K.; Haria, M.; Meisel, D.; Kamat, P. *Nano Lett.* **2004**, *4*, 415.
(29) Pierson, H. O. *Handbook of Chemical Vapor Deposition*; Noyes Publications: New York, 1992.
(30) Galasso, F. S. *Chemical Vapor Deposited Materials*; CRC Press Inc.: Boca Raton, FL, 1991.
(31) Serp, P.; Kalck, P. *Chem. Rev.* **2002**, *102*, 3085.
(32) Iwasawa, Y. In *Handbook of Heterogeneous Catalysis*; Ertl, G., Knozinger, H., Weitkamp, J., Eds.; Wiley-VCH: New York, 1997; p 853.
(33) Tungler, A.; Tarnai, T.; Hegedus, L.; Fodor, K.; Mathe, T. *Plantinum Metal Rev.* **1998**, *42*, 108.
(34) Blaser, H. U.; Indolese, A.; Schnyder, A.; Steiner, H.; Studer, M. *J. Mol. Catal. A* **2001**, *173*, 3.
(35) Toebes, M. L.; van Dillen, J. A.; de Jong, K. P. *J. Mol. Catal. A* **2001**, *173*, 75.
(36) Mehnert, C. P.; Weaver, D. W.; Ying, J. Y. *J. Am. Chem. Soc.* **1998**, *120*, 12289.
(37) Mehnert, C. P.; Ying, J. Y. *Chem. Commun.* **1997**, 2215.
(38) Mu, X.; Bartmann, U.; Guraya, M.; Busser, G. W.; Weckenmann, U.; Fischer, R.; Muhler, M. *Appl. Catal., A* **2003**, *248*, 85.
(39) Hierso, J. C.; Serp, P.; Feurer, R.; Kalck, P. *Appl. Organomet. Chem.* **1998**, *12*, 161.
(40) Feng, M. Q.; Puddephatt, R. J. *Can. J. Chem.* **2007**, *85*, 645.
(41) Serp, P.; Feurer, R.; Kihn, Y.; Kalck, P.; Faria, J. L.; Figueiredo, J. L. *J. Mater. Chem.* **2001**, *11*, 1980.
(42) Serp, P.; Feurer, R.; Kihn, Y.; Kalck, P.; Faria, J. L.; Figueiredo, J. L. *J. Phys. IV* **2002**, *12*, 29.
(43) Liang, C. H.; Xia, W.; Soltani-Ahmadi, H.; Schlüter, O.; Fischer, R.; Muhler, M. *Chem. Commun.* **2005**, 282.
(44) Zhang, Y.; Yuan, Z.; Puddephatt, R. J. *Chem. Mater.* **1998**, *10*, 2293.
(45) Tatsuno, Y.; Seiotsuka, T. Y. *Inorg. Synth.* **1979**, *19*, 220.
(46) Hierso, J. C.; Satto, C.; Feurer, R.; Kalck, P. *Chem. Mater.* **1996**, *8*, 2481.

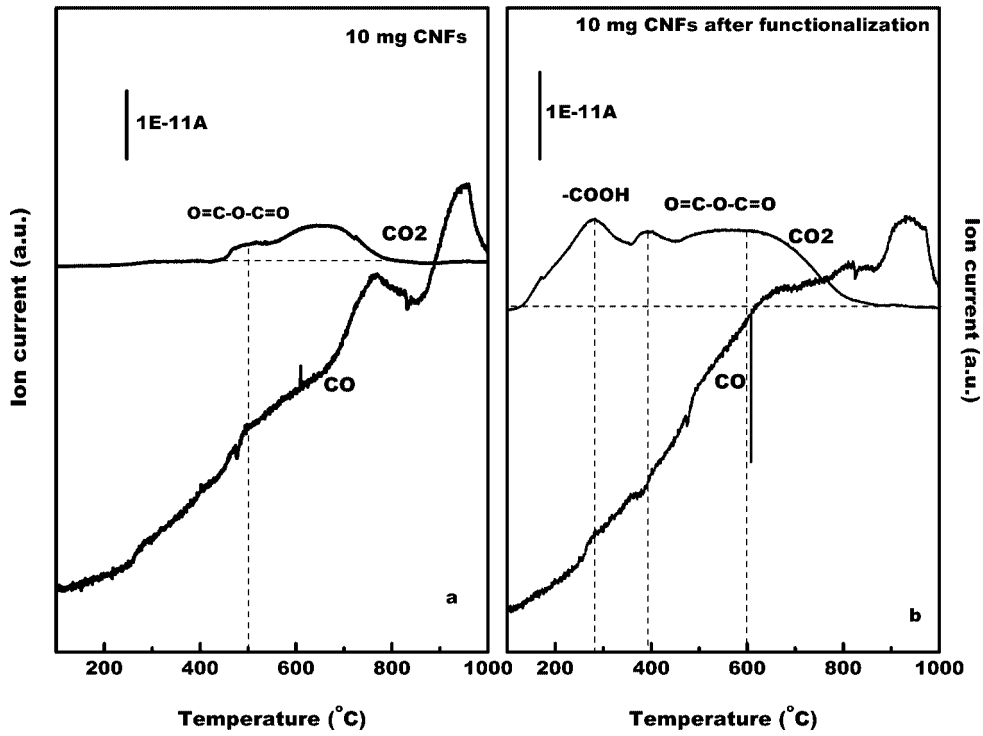

Figure 2. TPD-MS profiles of the raw CNFs (a) and the functionalized CNFs by treatment with HNO_3 solution (b) in helium.

The sublimator temperature was kept at 50 °C to fix the vapor pressure of the precursor. After adsorption, 30 vol % hydrogen in helium (with a flow rate of 70 mL min^{-1}) was added to reduce the adsorbed sample precursor. An online mass spectrometer (Balzers QMS 200) was set up on the reactor via a capillary tube to detect the fragmentation patterns during the CVD. The as-prepared samples were denoted as Pd-CNFs-1 to Pd-CNFs-4, depending on their Pd loadings from 0.17 to 4.3 wt %.

Temperature-programmed desorption (TPD) was carried out in helium with a flow rate of 100 mL min^{-1}. The sample was heated linearly at a rate of 10 °C/min from room temperature to 1000 °C. A Balzers QMS 200 mass spectrometer was used as detector.

The palladium content was determined by inductively coupled plasma−optical emission spectroscopy (ICP-OES). The samples were treated with sodium peroxide solution and then nitric acid solution, and the solution was filtered and analyzed by ICP-OES.

The crystalline phases and the palladium particle size were investigated by X-ray powder diffraction (XRD) on a Bruker-AXS D8 Advance using Cu Kα radiation ($\lambda = 0.154178$ nm) and a position sensitive detector.

XPS measurements were performed in a Scienta SES 2002 spectrometer using monochromated Al Kα radiation with 1486.6 eV. The X-ray source was operated at 14 kV and 55 mA in emission current. The pressure within the sample chamber was below 5×10^{-10} mbar. Survey spectra were recorded with a pass energy of 500 eV, whereas for the individual spectral lines 100 eV was used as pass energy. The step size for the regions was 100 meV. The calibration of the energy scale was made relative to the binding energy of C 1s at 285.0 eV.

Transmission electron microscopy (TEM) images and electron diffraction patterns were taken using a Phillips CM200 FEG microscope operating at 200 kV. The samples were prepared by placing one drop of the alcohol suspension on a carbon film supported on a copper grid.

The catalytic hydrogenation of cyclooctene was carried out in a fixed-bed reactor at 40 °C under atmospheric pressure using N_2 as the carrier gas. The molar ratio of N_2 to H_2 to cyclooctene was 100:1:1. The catalyst weight was about 25 mg to avoid full conversion. The total flow rate amounted to 300 cm^3 min^{-1} (STP). The composition of the reactor effluent was analyzed by online gas chromatography using a Chrompack CP-WAX 52B column and a flame ionization detector.

Results and Discussion

Surface Functionalization of the Raw CNFs. When the support was not functionalized by HNO_3, no palladium was detected by ICP-OES and no palladium particles were found by TEM after Pd deposition on the catalyst. Instead, deposition of Pd black was observed on the glass walls of the reactor because of the low amount of anchoring sites on the support, which is in agreement with phenomena observed during the deposition of platinum onto carbon nanospheres,[41] multiwalled CNTs, and graphite without treatment.[42] Therefore, it is essential for CNFs as catalyst support to introduce a number of anchoring sites on the materials.

Figure 2 shows the TPD-MS results of the raw CNFs and the functionalized CNFs. The types and the amount of surface oxygen-containing groups can be determined by the evolved CO ($m/e = 28$) and CO_2 ($m/e = 44$). For the raw CNFs, the CO_2 profile (Figure 2a) displayed two peaks at about 500 and 650 °C, while the CO profile exhibited one broad peak with a maximum at around 950 °C and a shoulder at 750 °C. The peak assignments of CO and CO_2 are summarized in Table 1 on the basis of the literature.[47−49] The first CO_2 peak at 500 °C can be attributed to anhydrides, and the peak

(47) Moreno-Castilla, C.; Ferro-Gacia, M. A.; Joly, J. P.; Bautist-Toledo, I.; Carrasco-Marin, F.; Rivera-Utrilla, J. *Langmuir* **1995**, *11*, 4386.
(48) Figueiredo, J. L.; Pereira, M. F. R.; Freitas, M. M. A.; Orfao, J. J. M. *Carbon* **1999**, *37*, 1379.
(49) Ros, T. G.; van Dillen, A. J.; Geus, J. W.; Koningsberger, D. C. *Chem.—Eur. J.* **2002**, *8*, 1151.

Table 1. Peak Assignments of the TPD-MS Profiles in Helium

peak	assignment	references
CO_2		
<300 °C	carboxylic acids	47−49
300−600 °C	carboxylic anhydrides	48, 49
>600 °C	lactones	48, 49
CO		
>600 °C	phenols, carbonyls, quinines, ethers	48, 49

at 650 °C may be tentatively assigned to lactones. For the CO evolution profile, the assignment of specific groups to peaks is difficult. In principle, CO could originate from phenol, carbonyl, quinine, and ether groups. The functionalized CNFs have a different TPD-MS profile (Figure 2b). It is obvious that three CO_2 peaks at around 300, 400, and 600 °C were observed and that the intensity is stronger than that of the raw CNFs. The CO_2 peak at below 300 °C may be attributed to carboxylic acid groups, while the CO_2 peaks at 400 and 600 °C may result from carboxylic anhydrides and lactones, respectively. The CO profile from the functionalized CNFs exhibited a broad range up to 1000 °C and is similar to the profile from the raw CNFs, but with high intensity, indicating an increase of phenols with high thermal stability after the functionalization of the CNFs. An increase in the amount of oxygen-containing groups is evidenced by the increase of the CO and CO_2 peaks after the functionalization. The results are in agreement with the data on functionalized CNFs obtained from HNO_3 solution treatment in refs 49 and 50.

Figure 3 shows XPS spectra of the raw CNFs and the CNFs functionalized with HNO_3 solution. Both samples exhibited a large peak around 285.0 eV, which can be attributed to the sp^2 carbon atoms of the carbon skeleton. However, there are some differences in the spectra from the two samples. Another weak peak from the CNFs functionalized with HNO_3 solution is observed at about 289.0 eV;

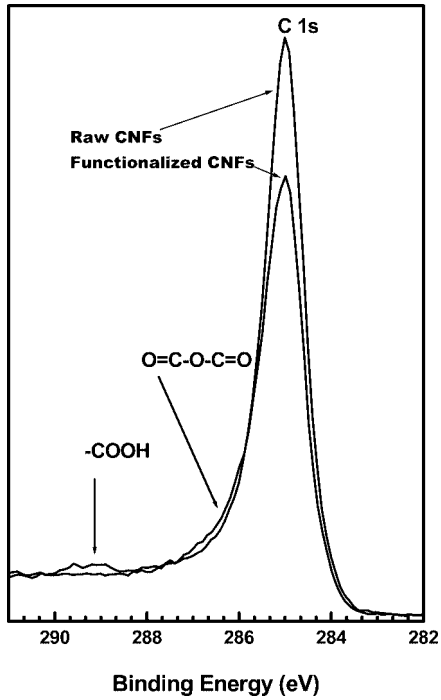

Figure 3. XPS spectra of the raw CNFs and the functionalized CNFs by treatment with HNO_3 solution.

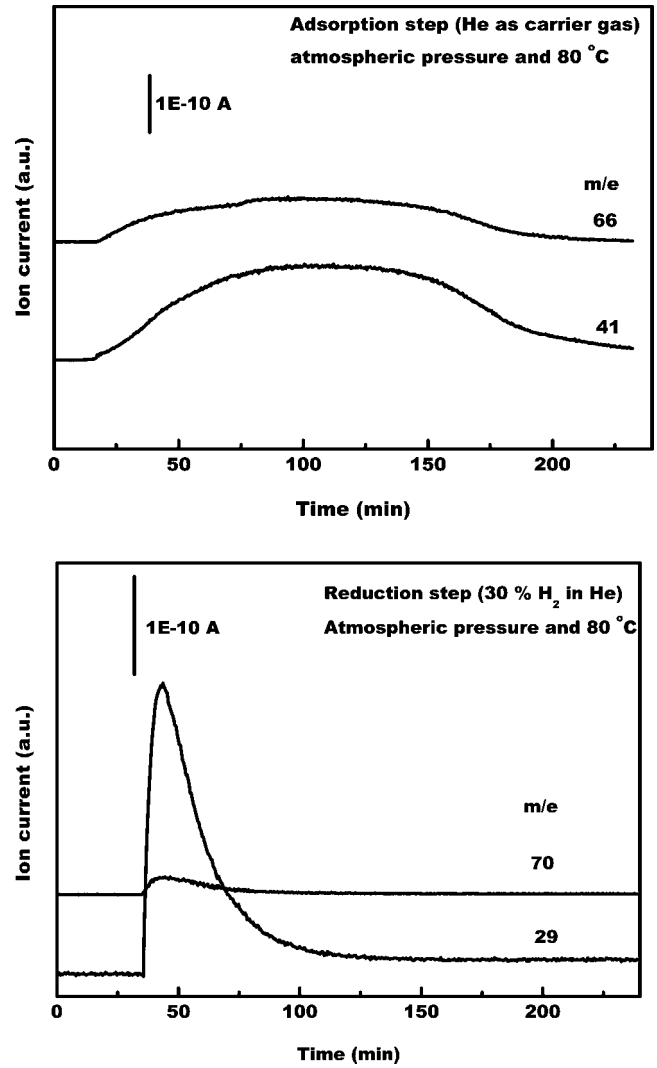

Figure 4. Mass spectroscopy data obtained during adsorption of the Pd(allyl)(Cp) precursor in He, followed by reduction with 30 vol % H_2/He.

the peak is broad on its high energy side (286−287 eV). The peak at about 289.0 eV and the broad peak in the range of 286−287 eV can be tentatively assigned to carbon atoms having a total of three bonds to oxygen atoms (−COO−) and carbon atoms singly coordinated to an oxygen atom (−OH, −C−O−C−).[51,52] Kundu et al. deconvoluted the C 1s spectrum of the oxidized carbon nanotubes into the following bonds: carbon in graphite, carbon single bound to oxygen in phenols and ethers, carbon doubly bound to oxygen in ketones and quinones, carbon bound to two oxygens in carboxyls, carboxylic anhydrides, and ethers, and the characteristic shakeup line of carbon in aromatic compounds.[53] The results provide evidence that surface oxygen groups (carboxylic acid groups, anhydride, and phenols) were introduced onto the surface of CNFs by the HNO_3 functionalization.

(50) Sainsbury, T.; Fitzmaurice, D. *Chem. Mater.* **2004**, *16*, 2174.
(51) Yue, Z. R.; Jiang, W.; Wang, L.; Toghiani, H.; Gardner, S. D.; Pittman, C. U., Jr. *Carbon* **1999**, *37*, 1607.
(52) Haiber, H.; Ai, X.; Bubert, H.; Heintze, M.; Brüser, V.; Brandl, W.; Marginean, G. *Anal. Bioanal. Chem.* **2003**, *375*, 875.
(53) Kundu, S.; Wang, Y. M.; Xia, W.; Muhler, M. *J. Phys. Chem. C* **2008**, *112*, 16869.

Scheme 1. Surface Functionalization of CNFs Followed by the Two-Step CVD of Pd(allyl)(Cp)

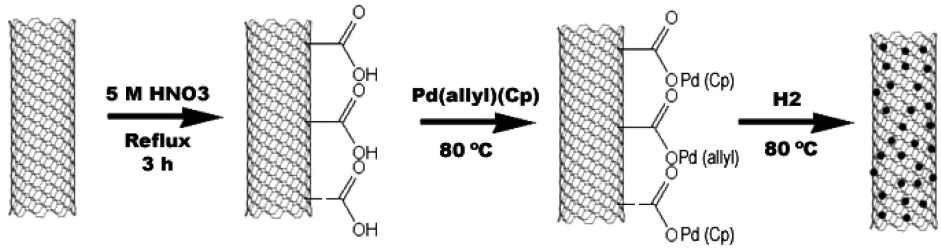

Table 2. Pd/CNF nanocomposite catalysts prepared by the two-step CVD method

sample	Pd contents by ICP-OES (wt %)	Pd particle sizes by TEM (nm)
Pd/CNFs-1	0.17	
Pd/CNFs-2	2.04	2−3
Pd/CNFs-3	3.22	3−4
Pd/CNFs-4	4.30	3−4

Taking both the TPD and XPS results into consideration, we conclude that a number of surface oxygen groups (carboxylic acid groups, anhydride, and phenols) were introduced on the CNFs surface after the functionalization with HNO_3 solution and that phenol groups showed high thermal stability.

CVD of Pd(allyl)(Cp) onto the Functionalized CNFs. The CVD of Pd(allyl)(Cp) onto the functionalized CNFs was achieved by a two-step process at atmospheric pressure. The process was studied by online mass spectroscopy taking the fragmentation patterns into account. Figure 4a shows the mass spectroscopic profile during adsorption of Pd(allyl)(Cp) on the functionalized CNFs at 80 °C. Simultaneously observed is the formation of cyclopentadiene ($m/e = 66$) and propene ($m/e = 41$). The thermolysis of Pd(allyl)(Cp) in the absence of any reactive gas was reported to give a mixture of propene, cyclopentadiene, and traces of hexadiene, which is consistent with mainly a radical mechanism.[54] The Pd(allyl)(Cp) precursor begins to decompose at 260 °C in the presence of helium under a pressure of 50 Torr.[46] Under our conditions, the formation of cyclopentadiene and propene comes from the dissociative adsorption of the Pd(allyl)(Cp) on the surface of the functionalized CNFs. The TPD-MS and XPS results provide evidence that surface oxygen groups (carboxylic acid groups, anhydride, and phenols) were introduced to the surface of CNFs by the HNO_3 functionalization. These surface oxygen groups are assumed to be mainly responsible for the dissociative adsorption of the precursor replacing the roughly equally strongly bound allyl and Cp ligands. Obviously, it depends on the reactivity of the surface oxygen groups as to which ligand is dissociated off, because the Pd−Cp and Pd−allyl bond dissociation energies are close.[55] On silica and MCM-41, hydroxyl groups are considered as the anchoring sites of Pd(allyl)(Cp) since only cyclopentadiene was detected during the adsorption.[36−39]

During the reduction step (Figure 4b), cyclopentane ($m/e = 70$) and propane ($m/e = 29$) were obtained simultaneously. The $m/e = 70$ was chosen as the characteristic fragment of cyclopentane because the pattern was only from fragments of cyclopentane. However, at present it is not possible to decide whether the alkanes originate from hydrogen-assisted elimination or from subsequent olefin hydrogenation over metallic Pd particles within the fixed bed. During the one-step CVD of Pd(allyl)(Cp), Hierso et al. observed an immediate decrease of the concentration of alkanes and an increase in the concentrations of alkenes after the H_2 was cut off, and the concentrations of the species rapidly restored the initial values as soon as H_2 was reintroduced into the reactor.[39,46] In comparison to thermolysis of the precursor at near 400 °C without reactive gas, the mechanism at low temperature is considered as autocatalytic decomposition on the support surface. Large palladium particles or thin films were generally formed in the one step CVD.

Considering the surface functionalization of CNFs and the two-step CVD of Pd(allyl)(Cp), the preparation of Pd/CNF nanocomposites can be depicted as indicated in Scheme 1. First, CNFs were functionalized with HNO_3 solution. A number of carboxylic groups were formed as the anchoring sites of metal precursor. Second, the Pd(allyl)(Cp) precursor adsorbed dissociatively on the surface of the CNFs by the reaction between the ligands and the carboxylic groups. Finally, the precursor adsorbed on the CNFs was further reduced in H_2, and the Pd/CNF nanocomposites were obtained.

Characterization of Pd Nanoparticle/Functionalized CNF Composites. Table 2 lists the palladium loading in the Pd/CNFs nanocomposites, as obtained from ICP-OES. The palladium loadings are between 0.17 and 4.3 wt %. The level of Pd loading depended on the degree of functionalization

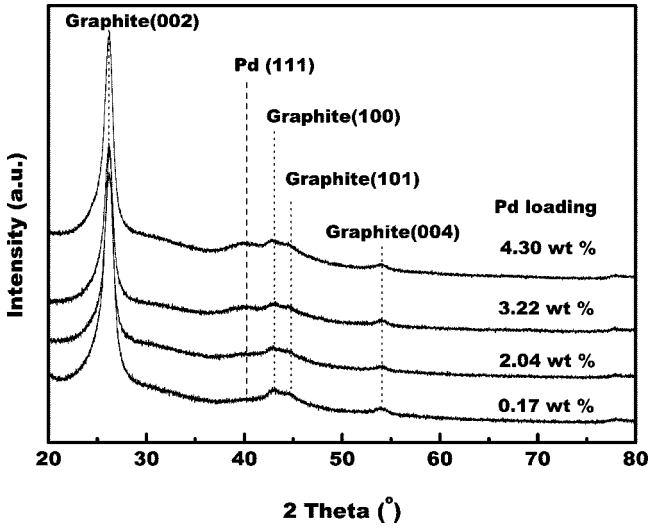

Figure 5. XRD patterns of Pd particles supported on the functionalized CNFs.

(54) Gozum, J. E.; Pollina, D. M.; Jensen, J. M.; Girolami, G. S. *J. Am. Chem. Soc.* **1988**, *110*, 2688.

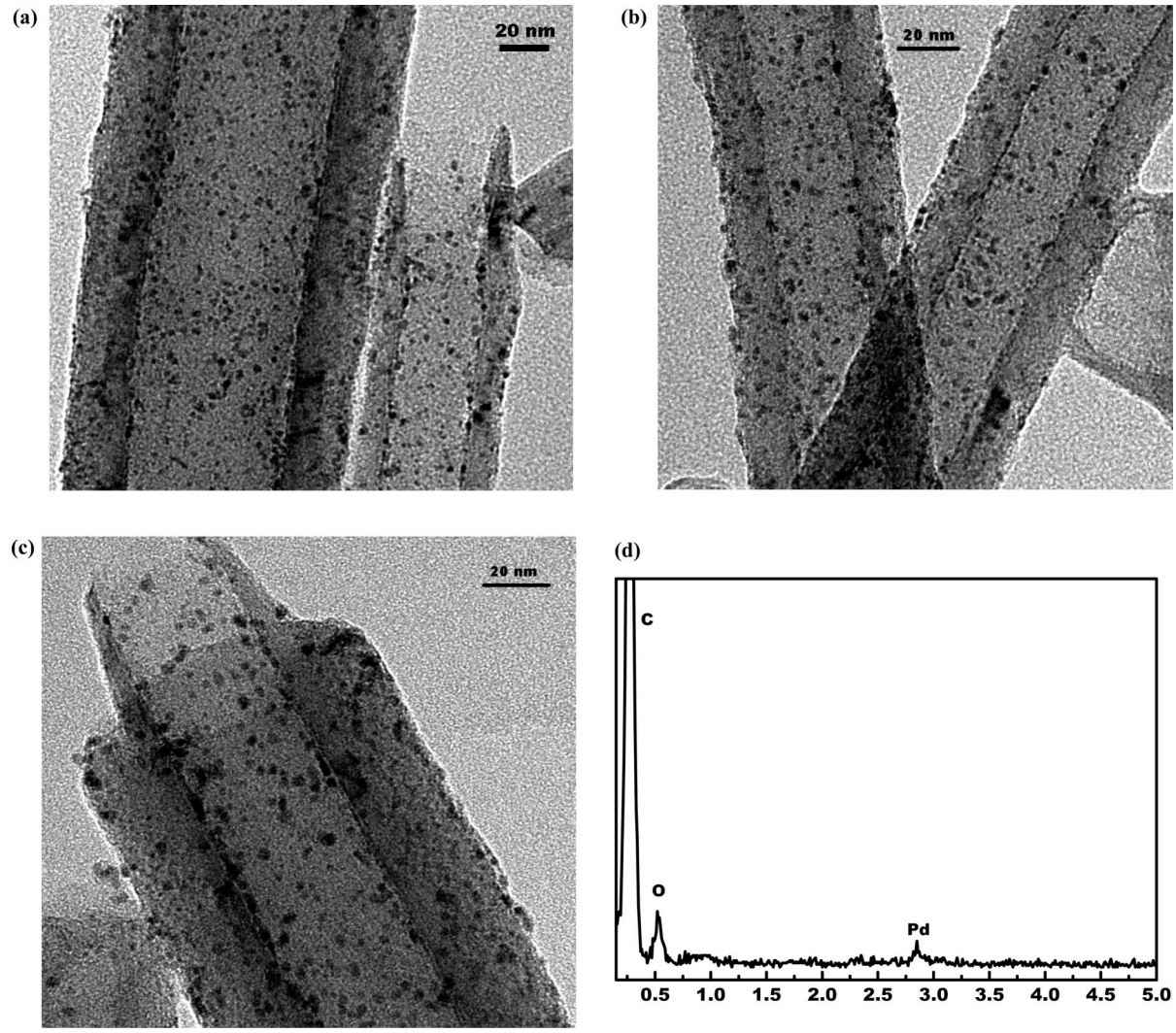

Figure 6. TEM images and EDX analysis of Pd particles supported on the functionalized CNF composites. 2.04% Pd/CNFs (a); 3.22% Pd/CNFs (b); 4.30% Pd/CNFs (c); EDX analysis of 2.04% Pd/CNFs (d).

Scheme 2. Catalytic Hydrogenation of Cyclooctene

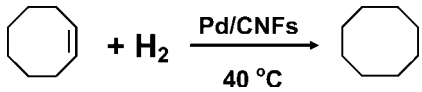

of the CNFs and on the amount of precursor provided in the sublimation chamber. When the support was not functionalized by HNO_3 solution, no palladium was detected by ICP-OES. Therefore, the surface functionalization of CNFs is an essential step to CVD of Pd from Pd(allyl)(Cp) onto CNFs.

X-ray diffraction (XRD) patterns of the Pd/CNFs nanocomposites shown in Figure 5 only reveal a broad Pd(111) diffraction peak at about $2\theta = 40.2°$ indicating rather small Pd particles, in addition to the diffraction peaks at 26.5, 42.4, 54.7, and 77.4°, originating from the hexagonal graphite structure (002), (100), (004), and (110) in the CNFs.

Figure 6 shows TEM images of the Pd/CNFs nanocomposites with palladium loading of 2.03 wt %, 3.22 wt %, and 4.30 wt %, respectively. Highly dispersed and evenly distributed Pd particles with diameters of 2−4 nm are observed on the three samples. The distribution of palladium particle sizes is summarized in Table 2. The high degree of dispersion points to a strong interaction between the metal precursor and the CNFs, resulting in a large number of Pd nuclei. Similar observations were reported by Pham-Huu et al.[16] for carbon nanofiber-supported Pd catalysts and by Park and Baker[17] for graphite nanofiber-supported Ni catalysts synthesized by incipient wetness impregnation. However, the distribution of the metal particles achieved in this way was relatively broad, ranging from 1 to 11 nm for Pd and from 1.5 to 43.5 nm for Ni, compared with the distribution in the range from 2 to 4 nm, clearly demonstrating the advantages of CVD in the preparation of the supported catalysts. In addition, energy dispersive analysis by EDX on the sample with palladium loading of 2.03 wt % indicated that palladium was highly dispersed on the CNFs (Figure 6d).

The Pd/CNF nanocomposites were used to catalyze the hydrogenation of cyclooctene (Scheme 2). The reaction was carried out in fixed bed reactor at 40 °C under atmospheric pressure. The catalytic activities of the catalysts are shown in Figure 7. The conversions were very stable over the four catalysts, which is a significant improvement over catalysts

(55) Stauf, G. T.; Dowben, P. A.; Emrich, K.; Barfuss, S.; Hirschwald, W.; Boag, N. M. *J. Phys. Chem.* **1989**, *93*, 749.

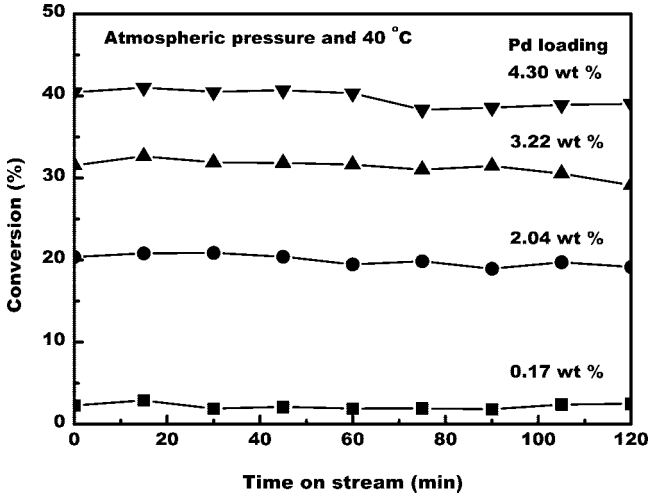

Figure 7. Hydrogenation of cyclooctene over Pd particles supported on the functionalized CNF composites.

prepared by the impregnation route. Jackson et al.[56] studied the hydrogenation of cycloalkenes on supported palladium catalysts prepared by the impregnation route and observed rapid deactivation in the initial stage, which was attributed to the formation of a carbonaceous layer on the palladium surface. It is worth noting that no activity for cyclooctene hydrogenation was observed on the activated carbon supported palladium catalyst. Okhlopkova et al.[57,58] reported that the hydrogenation rate of cyclooctene is low on the Pt/C catalysts produced by the impregnation method. They also found that the catalytic activities decreased upon decreasing the dimension of the micropores in the support and the size of the metal particles, confirming the complete blocking of part of the metal surface in narrow pores. In our experiments, the superior activity can be attributed to the special interaction between the palladium nanoparticles and the CNFs, which has also been observed for Ni/CNFs[16] and Ru/CNFs.[14,18] In addition, the open structure of a fixed bed consisting of non-microporous CNFs is beneficial to avoid mass transfer limitations. It can also be seen that the conversions were almost in proportion to the palladium loading, which further confirms that the particle size on the Pd/CNFs is the same for the four samples with different loadings.

Conclusions

The two-step CVD method can be used to synthesize highly dispersed Pd nanoparticles supported on CNFs under mild conditions. The functionalization of CNFs is a necessary step to provide anchoring sites by treatment with HNO_3 solution. The two-step CVD of the Pd(allyl)(Cp) on the functionalized CNFs involves the dissociative adsorption on the surface of the CNFs by the reaction between the ligands and the surface oxygen groups and the reduction in H_2 to the Pd/CNFs nanocomposites. The Pd/CNF nanocomposite catalysts showed high activity and stability in the hydrogenation of cyclooctene, presumably a result of special metal−support interactions and the absence of micropores. The two-step CVD route is of great potential in the controlled synthesis of carbon nanofiber-supported metal catalysts with high dispersion and uniform distribution.

Acknowledgment. We acknowledge the financial support from the Deutsche Forschungsgemeinschaft. C.L. is indebted to the Alexander von Humboldt Stiftung for a fellowship.

CM8031225

(56) Jackson, S. D.; Kelly, G. J.; Watson, S. R.; Gulickx, R. *Appl. Catal., A* **1999**, *187*, 161.
(57) Okhlopkova, L. B.; Lisitsyn, A. S.; Boehm, H. P.; Likholobov, V. A. *Rect. Kinet. Catal. Lett.* **2000**, *71*, 165.
(58) Okhlopkova, L. B.; Lisitsyn, A. S.; Likholobov, V. A.; Gurrath, M.; Boehm, H. P. *Appl. Catal., A* **2003**, *204*, 229.